Thai Journal of Mathematics
Volume 7 (2009) Number 1 : 171–187

www.math.science.cmu.ac.th/thaijournal
Online ISSN 1686-0209

Numerical solutions of flows under an inclined gate

P. Guayjarernpanishk and J. Asavanant

Abstract : Two-dimensional free-surface flows of an inviscid and incompressible fluid under an inclined gate is considered. The flow is assumed to be steady and irrotational. This problem is solved numerically by using boundary integral equation technique. Numerical results for inclined gate are presented for various values of the gate inclination γ and the gate length L when the upstream free surface separates at a stagnation point. These solutions can be found for certain values of γ, that is, $\chi_L < \gamma \leq 90°$. Here χ_L is the lower bound for gate inclination depending on the gate length L and the corresponding downstream Froude number. As the gate length decreases, nonlinear effect on the upstream waves is apparent so that the waves tend to develop narrow crests and broad troughs. When the upstream free-surface separates tangentially from the gate, the so-called *smooth attachment*, it is found that there exist solutions for larger values of gate inclination. As L increases, the elevation of the crests tends to the maximum level and the waves ultimately reach their limiting configuration characterized by a 120° angle at the crests.

Keywords : Free-surface flow, inclined gate, boundary integral equation.

2000 Mathematics Subject Classification : 76B07

1 Introduction

Free-surface flow under a gate is one of the well-known classical problem in fluid mechanics. Analytical and numerical results have been proposed for different flow configurations by many researchers. Free-streamline solutions of flow under a gate were studied by Lord Rayleigh in the mid nineteenth century. He neglected the effect of gravity and solved by using conformal transformations. Later on, numerical solutions of free-surface flows under a gate with the effect of gravity

were presented by Southwell and Vaisey (1946). In 1952, Binnie suggested the use of nondimensional parameter, the Froude number F, and gave a tentative argument indicating that waves cannot be present on the downstream side of the gate. Approximate analytic solutions were derived by Benjamin (1956), using the theories of jets and solitary wave, and compared with experimental results for the same gate opening. Cheng and et al. (1981) was among others to formulate the problem by using boundary integral equation technique and to achieve relatively good solution accuracy.

Vanden-Broeck (1986) computed numerical solutions of flow under a gate without upstream free surface by the method of series truncation. He found that there are two solutions for $1.80 \leq F \leq 1.87$, one solution for $F > 1.87$, and no solutions for $F < 1.80$. Here F is the downstream Froude number. In 1996, Asavanant and Vanden-Broeck considered the complete sluice gate problem with two free surfaces and constructed solutions for which the free surface leave tangentially at both separation points by series truncation procedure. Their results could be obtained only for small values of gate inclination γ. Vanden-Broeck (1997) computed numerical solution for the fully nonlinear vertical gate problem using boundary integral equation technique. He showed that there exist solutions for which the flow does not satisfy the upstream uniform flow condition. These solutions are characterized by a train of waves on the upstream free surface. Analytic solution of the smooth attachment problem was presented implicitly as an integral equation by Petrila (2002). He reduced the problem to a boundary value problem of the Hilbert type and employed Muskelishvili's technique without solving for numerical solutions. In 2005, Binder and Vanden-Broeck considered both fully nonlinear and weakly nonlinear of the inclined gate problem. They introduced a new parameter to classify behavior of flow at the separation point between the upstream free-surface and the gate without showing the relationship between parameters.

In this paper, we consider fully nonlinear problem of the steady free-surface flows under an inclined gate with possibilities of either a stagnation point or a smooth attachment to occur at the separation point. Formulation of the problem and numerical procedure for flow under an inclined gate are given in § 2 and § 3, respectively. In § 4 we discuss the numerical results of free-surface flows under an inclined gate with stagnation point. The case in which the free surfaces leave tangentially at both separation points, smooth attachment, is discussed in § 5. Finally, concluding remarks are presented in § 6.

2 Mathematical Formulation

We consider the steady two-dimensional flow of an inviscid and incompressible fluid under an inclined gate. The flow is assumed to be irrotational. Fluid domain is bounded below by a horizontal rigid wall $A'D'$ and above by the free surfaces AB and CD and the gate BC (see Figure 1).

Let us introduce Cartesian coordinates with the x-axis along the bottom and the y-axis directed vertically upwards through the upstream separation point B.

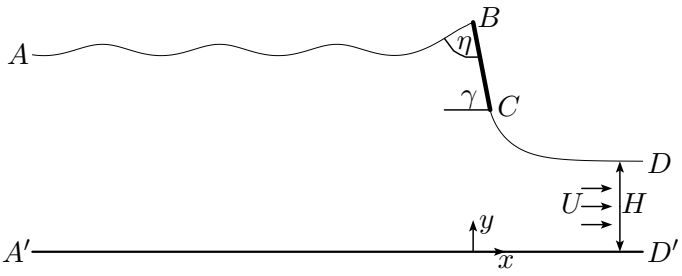

Figure 1: Sketch of the flow domain in the physical plane.

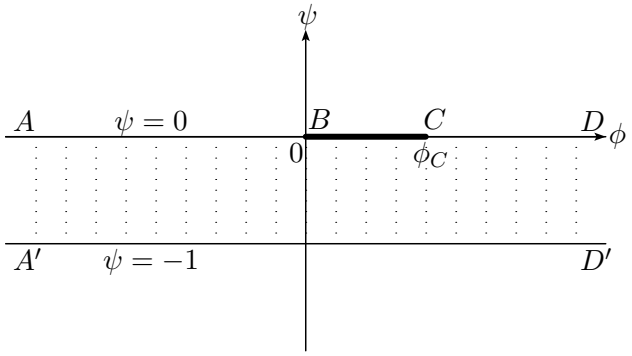

Figure 2: Fluid domain in the complex potential f-plane.

Hence, gravity g acts in the negative y-direction. The gate inclination is denoted by γ measured clockwise from the negative x-axis. At B, we denote by η the angle between free surface and gate. The flow is subcritical far upstream and supercritical far downstream. As $x \to \infty$, the flow is assumed to approach a uniform stream with constant velocity U and constant depth H. It is convenient to define dimensionless variables by taking U as the unit velocity and H as the unit length.

Let's introduce the velocity potential $\phi(x, y)$ and the stream function $\psi(x, y)$ by defining the complex potential function f as

$$f = \phi(x, y) + i\psi(x, y).$$

The complex velocity w can be written as

$$w = \frac{df}{dz} = u - iv,$$

where u and v are the velocity components in the x and y directions, and $z = x+iy$. Without loss of generality, we choose $\phi = 0$ at B and $\psi = 0$ on the free surfaces AB, CD and on the gate BC. The bottom $A'D'$ defines another streamline on which $\psi = -UH$. By the choice of our dimensionless variables, we have $\psi = -1$ on the

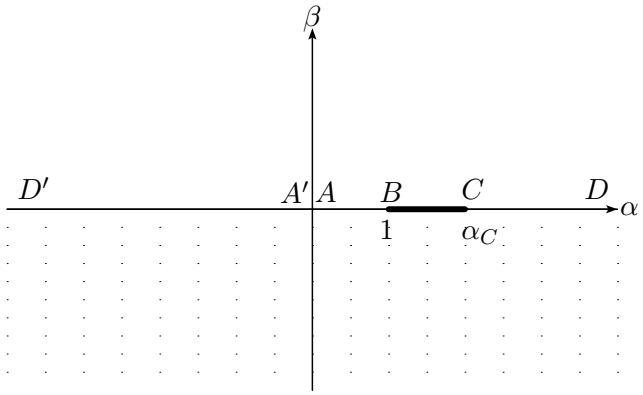

Figure 3: Flow domain in the lower half of complex ζ-plane.

bottom $A'D'$. We denote the value of the potential function at the downstream separation point C by ϕ_C. Figure 2 depicts the fluid domain in the complex potential f-plane.

In terms of the dimensionless veriables, the nonlinear free surface condition for this problem can be expressed in terms of the *Bernoulli equation* as

$$u^2 + v^2 + \frac{2}{F^2}(y-1) = 1, \tag{2.1}$$

where F is the Froude number defined by $F = \frac{U}{\sqrt{gH}}$. The kinematic boundary condition on the bottom $A'D'$ and the gate BC can be written as

$$v = 0 \quad \text{on} \quad \psi = -1 \quad \text{and} \quad -\infty < \phi < \infty, \tag{2.2}$$

and

$$v = -u\tan\gamma \quad \text{on} \quad \psi = 0 \quad \text{and} \quad 0 < \phi < \phi_C. \tag{2.3}$$

This concludes the mathematical formulation of the problem. We seek w as an analytic function of f in the strip $-1 < \psi < 0$ such that $w \to 1$ as $\phi \to \infty$ and (2.1) - (2.3) are satisfied.

We map the flow domain from the complex potential f-plane onto the lower half of complex ζ-plane by using the conformal mapping

$$\zeta = \alpha + i\beta = e^{\pi f} \tag{2.4}$$

as shown in Figure 3.
Next we introduce the new complex function $\tau - i\theta$ by

$$w = e^{\tau - i\theta}. \tag{2.5}$$

To construct an integral equation for this problem, we apply the Cauchy's integral formula to the function $\tau - i\theta$ in the complex ζ-plane with a contour consisting of

the real axis α and the circumference of a half circle of arbitrary large radius in the lower half plane. After taking the real part, we obtain

$$\tau(\alpha) = \frac{1}{\pi}\int_{-\infty}^{\infty} \frac{\theta(\alpha')}{\alpha' - \alpha} d\alpha' \quad \text{on} \quad \beta = 0, \tag{2.6}$$

where $\tau(\alpha)$ and $\theta(\alpha)$ denote the value of τ and θ on the free surfaces.

The kinematic boundary conditions (2.2) and (2.3) become

$$\theta(\alpha) = 0 \quad \text{for} \quad \beta = 0 \quad \text{and} \quad \alpha < 0, \tag{2.7}$$

and

$$\theta(\alpha) = -\gamma \quad \text{for} \quad \beta = 0 \quad \text{and} \quad 1 < \alpha < \alpha_C, \tag{2.8}$$

where $\alpha_C = e^{\pi\phi_C}$. Substituting (2.7) and (2.8) into (2.6), we obtain

$$\tau(\alpha) = -\frac{\gamma}{\pi} \ln \frac{|\alpha_C - \alpha|}{|1 - \alpha|} + \frac{1}{\pi}\int_0^1 \frac{\theta(\alpha')}{\alpha' - \alpha} d\alpha' + \frac{1}{\pi}\int_{\alpha_C}^{\infty} \frac{\theta(\alpha')}{\alpha' - \alpha} d\alpha'. \tag{2.9}$$

Equation (2.9) provides a relation between τ and θ on the free surfaces. Another relation between τ and θ on the free surfaces can be found from equation (2.1) as

$$e^{2\tau} + \frac{2}{F^2}(y - 1) = 1. \tag{2.10}$$

Using (2.4) and integrating the identity

$$\frac{d}{df}(x + iy) = w^{-1}, \tag{2.11}$$

we can find the downstream free surface displacement from

$$x(\alpha) = \frac{1}{\pi}\int_1^{\alpha} \frac{e^{-\tau(\alpha')}}{\alpha'} \cos\theta(\alpha') d\alpha', \tag{2.12}$$

$$y(\alpha) = 1 + \frac{F^2}{2}(1 - e^{2\tau(\alpha_B)}) + \frac{1}{\pi}\int_1^{\alpha} \frac{e^{-\tau(\alpha')}}{\alpha'} \sin\theta(\alpha') d\alpha' \tag{2.13}$$

for $0 < \alpha < 1$ and the upstream free surface displacement from

$$x(\alpha) = x_C + \frac{1}{\pi}\int_{\alpha_C}^{\alpha} \frac{e^{-\tau(\alpha')}}{\alpha'} \cos\theta(\alpha') d\alpha', \tag{2.14}$$

$$y(\alpha) = 1 + \frac{1}{\pi}\int_{\infty}^{\alpha} \frac{e^{-\tau(\alpha')}}{\alpha'} \sin\theta(\alpha') d\alpha' \tag{2.15}$$

for $\alpha > \alpha_C$, where x_C is the position of separation point C.

Equations (2.9), (2.10) and (2.12) - (2.15) define a system of nonlinear integral equations for the unknowns $\theta(\alpha)$ on the free surfaces $0 < \alpha < 1$ and $\alpha > \alpha_C$.

3 Numerical procedure

The above system of nonlinear equations is solved numerically by using equally spaced points in the potential function ϕ. Introducing the change of variables

$$\alpha = e^{\pi\phi}$$

on free surfaces, we can rewrite (2.9) as

$$\bar{\tau}(\phi) = -\frac{\gamma}{\pi}\ln\frac{|e^{\pi\phi_C} - e^{\pi\phi}|}{|1 - e^{\pi\phi}|} + \int_{-\infty}^{0}\frac{\bar{\theta}(\phi_0)e^{\pi\phi_0}}{e^{\pi\phi_0} - e^{\pi\phi}}d\phi_0 + \int_{\phi_C}^{\infty}\frac{\bar{\theta}(\phi_0)e^{\pi\phi_0}}{e^{\pi\phi_0} - e^{\pi\phi}}d\phi_0. \quad (3.1)$$

Accordingly, equations (2.10), (2.12) - (2.15) can be rewritten as follows

$$e^{2\bar{\tau}(\phi)} + \frac{2}{F^2}(\bar{y}(\phi) - 1) = 1, \quad (3.2)$$

$$\bar{x}(\phi) = \int_0^{\phi} e^{-\bar{\tau}(\phi_0)}\cos\bar{\theta}(\phi_0)d\phi_0, \quad (3.3)$$

$$\bar{y}(\phi) = 1 + \frac{F^2}{2}(1 - e^{2\bar{\tau}(\phi_B)}) + \int_0^{\phi} e^{-\bar{\tau}(\phi_0)}\sin\bar{\theta}(\phi_0)d\phi_0, \quad (3.4)$$

for $-\infty < \phi < 0$, and

$$\bar{x}(\phi) = x_C + \int_{\phi_C}^{\phi} e^{-\bar{\tau}(\phi_0)}\cos\bar{\theta}(\phi_0)d\phi_0, \quad (3.5)$$

$$\bar{y}(\phi) = 1 + \int_{\infty}^{\phi} e^{-\bar{\tau}(\phi_0)}\sin\bar{\theta}(\phi_0)d\phi_0, \quad (3.6)$$

for $\phi_C < \phi < \infty$. Here $\bar{\tau}(\phi) = \tau(e^{\pi\phi})$, $\bar{\theta}(\phi) = \theta(e^{\pi\phi})$, $\bar{x}(\phi) = x(e^{\pi\phi})$ and $\bar{y}(\phi) = y(e^{\pi\phi})$.

Next we introduce equally spaced mesh points in the potential function ϕ by

$$\phi_I^U = -(I-1)\Delta_1, \qquad I = 1, ..., N_1$$

and

$$\phi_I^D = \phi_C + (I-1)\Delta_2, \qquad I = 1, ..., N_2$$

on the upstream and downstream free surfaces. Here $\Delta_1 > 0$ and $\Delta_2 > 0$ are the mesh sizes on upstream and downstream free surfaces, respectively. The corresponding unknowns are $F, \{\bar{\theta}(\phi_I^U)\}_{I=1}^{N_1}$ and $\{\bar{\theta}(\phi_I^D)\}_{I=1}^{N_2}$. For simplicity, we denote $\theta_I^U = \bar{\theta}(\phi_I^U)$ and $\theta_I^D = \bar{\theta}(\phi_I^D)$.

We assign the values $\theta_1^U = \delta$ and $\theta_1^D = -\gamma$, where δ will be defined later. There are $N_1 + N_2 - 1$ unknowns: $F, \{\theta_I^U\}_{I=2}^{N_1}$ and $\{\theta_I^D\}_{I=2}^{N_2}$. We evaluate the values $\tau_{I+\frac{1}{2}}^U$ and $\tau_{I+\frac{1}{2}}^D$ of $\bar{\tau}(\phi)$ at the midpoints

$$\phi_{I+\frac{1}{2}}^U = \frac{\phi_I^U + \phi_{I+1}^U}{2}, \qquad I = 1, ..., N_1 - 1$$

and

$$\phi^D_{I+\frac{1}{2}} = \frac{\phi^D_I + \phi^D_{I+1}}{2}, \qquad I = 1, ..., N_2 - 1$$

by applying the trapezoidal rule to the first and second integrals in (3.1) with summations over the ϕ^U_I and ϕ^D_I, respectively. The symmetry of the quadrature and of the distribution of mesh points enables us to evaluate the Cauchy principal values as if they were ordinary integrals. Then we replace (3.1) by

$$\bar{\tau}(\phi) = -\frac{\gamma}{\pi} \ln \frac{|e^{\pi\phi_C} - e^{\pi\phi}|}{|1 - e^{\pi\phi}|} + \int_{\phi^U_{N_1}}^{0} \frac{\bar{\theta}(\phi_0)e^{\pi\phi_0}}{e^{\pi\phi_0} - e^{\pi\phi}} d\phi_0 + \int_{\phi_C}^{\phi^D_{N_2}} \frac{\bar{\theta}(\phi_0)e^{\pi\phi_0}}{e^{\pi\phi_0} - e^{\pi\phi}} d\phi_0. \quad (3.7)$$

Following Hocking and Vanden-Broeck (1997), the last integral in (3.7) can be rewritten for computational purpose as

$$\int_{\phi_C}^{\phi^D_{N_2}} \frac{\bar{\theta}(\phi_0)e^{\pi\phi_0}}{e^{\pi\phi_0} - e^{\pi\phi}} d\phi_0 = \int_{\phi_C}^{\phi^D_{N_2}} \frac{(\bar{\theta}(\phi_0) - \bar{\theta}(\phi))e^{\pi\phi_0}}{e^{\pi\phi_0} - e^{\pi\phi}} d\phi_0 + \frac{\bar{\theta}(\phi)}{\pi} \ln \frac{|e^{\pi\phi^D_{N_2}} - e^{\pi\phi}|}{|e^{\pi\phi_C} - e^{\pi\phi}|} \quad (3.8)$$

before applying the trapezoidal rule. The values of $\bar{\theta}$ at the midpoints are evaluated using the four-point interpolation formula. Free surface profile can be determined directly from (3.3) - (3.6) as follows

$$x^U_I = \bar{x}(\phi^U_I) = \begin{cases} 0, & I = 1; \\ x^U_{I-1} - e^{(-\tau^U_{I-\frac{1}{2}})} \cos(\theta^U_{I-\frac{1}{2}})\Delta_1, & I = 2, 3, \ldots, N_1 \end{cases}$$

$$y^U_I = \bar{y}(\phi^U_I) = \begin{cases} 1 + \frac{1}{2}F^2(1 - e^{2\tau^U_1}), & I = 1; \\ y^U_{I-1} - e^{(-\tau^U_{I-\frac{1}{2}})} \sin(\theta^U_{I-\frac{1}{2}})\Delta_1, & I = 2, 3, \ldots, N_1 \end{cases}$$

where τ^U_1 is $\frac{3}{2}\tau^U_{1+\frac{1}{2}} - \frac{1}{2}\tau^U_{2+\frac{1}{2}}$, and

$$x^D_I = \bar{x}(\phi^D_I) = \begin{cases} x_C, & I = 1; \\ x^D_{I-1} + e^{(-\tau^D_{I-\frac{1}{2}})} \cos(\theta^D_{I-\frac{1}{2}})\Delta_2, & I = 2, 3, \ldots, N_2 \end{cases}$$

$$y^D_I = \bar{y}(\phi^D_I) = \begin{cases} y^D_{I+1} - e^{(-\tau^D_{I+\frac{1}{2}})} \sin(\theta^D_{I+\frac{1}{2}})\Delta_2, & I = N_2 - 1, N_2 - 2, \ldots, 1; \\ 1, & I = N_2 \end{cases}$$

We use y^U_I and y^D_I to evaluate $\bar{y}$ at the midpoints $\phi^U_{I+\frac{1}{2}}$ and $\phi^D_{I+\frac{1}{2}}$. We now satisfy (3.2) at the midpoints. This yields N_1+N_2-2 nonlinear algebraic equations for $N_1 + N_2 - 1$ unknowns. The last equation is obtained by fixing the length L of the gate BC. The final relation is then

$$L - \sqrt{(x^U_1 - x^D_1)^2 + (y^U_1 - y^D_1)^2} = 0. \quad (3.9)$$

For given values of ϕ_C and γ, we solve this system of $N_1 + N_2 - 1$ nonlinear algebraic equations with $N_1 + N_2 - 1$ unknowns by Newton's method.

4 Flows with a stagnation point

The above numerical procedure is used to find solution of free-surface flow under an inclined gate for given values of ϕ_C and γ. Accuracy of numerical solutions depends on the grid spacings, Δ_1 and Δ_2, and the domain truncations, N_1 and N_2. Most of the calculations are obtained with $N_1 = 841, N_2 = 501, \Delta_1 = 0.01$ and $\Delta_2 = 0.01$. We computed solutions for various values of Δ_1 and Δ_2, and N_1 and N_2 until the numerical solutions were in agreement within graphical accuracy. Figure 4 shows the effect of mesh size on the upstream free surface profile corresponding to $\phi_C = 0.26$ and $\gamma = 60^\circ$ for $\Delta_1 = 0.01$ and $\Delta_1 = 0.02$. This shows that our results are independent of Δ_1.

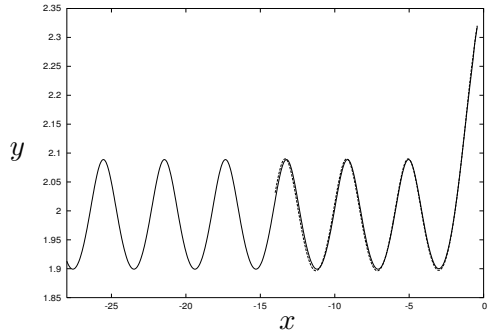

Figure 4: Profiles of the upstream free surface with $\Delta_1 = 0.01$ (dashed line) and $\Delta_1 = 0.02$ (solid line) for $\phi_C = 0.26$ and $\gamma = 60^\circ$.

Following Asavanant and Vanden-Broeck (1996), free-surface inclination at the stagnation point B can be described as

$$\eta = \begin{cases} 120^\circ, & 0^\circ \leq \gamma \leq 60^\circ; \\ 180^\circ - \gamma, & 60^\circ \leq \gamma \leq 90^\circ \end{cases}$$

and

$$\delta = \begin{cases} 60^\circ - \gamma, & 0^\circ \leq \gamma \leq 60^\circ; \\ 0^\circ, & 60^\circ \leq \gamma \leq 90^\circ. \end{cases}$$

Numerical solutions for gate inclination $0 < \gamma \leq 90^\circ$ are presented and discussed as follows.

4.1 Case of vertical gate ($\gamma = 90^\circ$)

This is the case considered by many investigators such as, Fangmeier and Strelkoff (1968), Naghdi and Vongsarnpigoon (1986), Vanden-Broeck (1997), Defina and Susin (2003). Here $\eta = 90^\circ, \delta = 0^\circ$. Typical free-surface profile is shown in Figure 5. It is found that the amplitude of upstream waves increases as ϕ_C decreases.

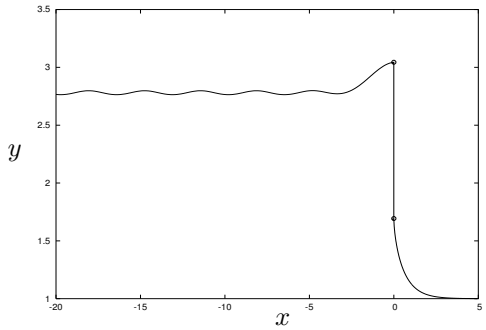

Figure 5: Profiles of the free surfaces and the gate when $\gamma = 90°, \phi_C = 0.26$ and $F = 2.0221$. The symbol $\circ$ indicates the end points of the gate at which separation occurs.

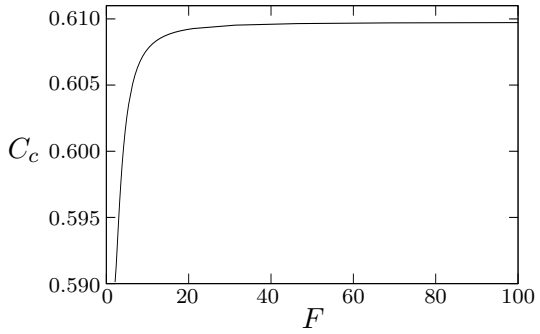

Figure 6: Values of the contraction coefficient C_c versus the Froude number F.

The contraction coefficient C_c, defined as the ratio of depth far downstream and gate opening, constitutes another important check on our numerical scheme. In case of zero gravity (Batchelor, 1967), the contraction coefficient for the free-streamline solution is given by

$$C_c^* = \frac{\pi}{\pi + 2} \approx 0.611015.$$

From our calculations, the numerical value of C_c differs from C_c^* by 0.21% (see Figure 6).

4.2 Case of inclined gate

4.2.1 $60° \leq \gamma < 90°$

In this case, the free-surface is horizontal in the neighborhood of stagnation point. That is, $\theta_1^U = \delta = 0°$. Typical free surface profiles for $\gamma = 70°$ is shown in Figure 7. It is found that there is a train of nonlinear waves on the upstream free-surface

similar to case of the vertical gate problem. For a given value of γ, the amplitude of upstream waves increases and the profiles develop broad troughs and narrow crests as ϕ_C decreases (see Figure 7 (b) - (d)). these wave ultimately reach the Stokes limiting configuration of 120° angle corner at the crests.

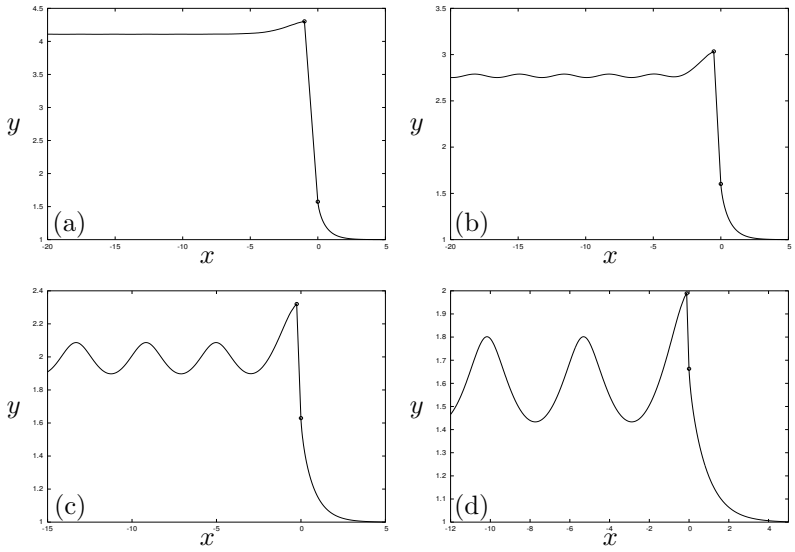

Figure 7: Profiles of the free surfaces and the gate when $\gamma = 70°$: (a) $\phi_C = 0.71$, $F = 2.5704$ (b) $\phi_C = 0.41$, $F = 2.0172$ (c) $\phi_C = 0.19$, $F = 1.6250$ and (d) $\phi_C = 0.075$, $F = 1.4064$.

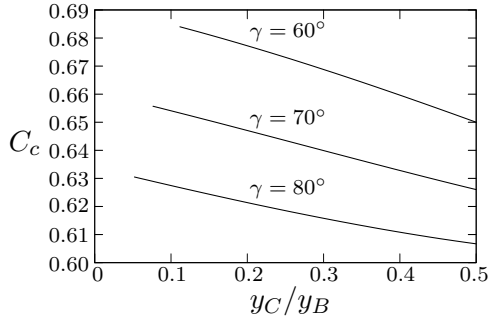

Figure 8: The contraction coefficient C_c versus $\frac{y_C}{y_B}$ for $\gamma = 80°, 70°$ and $60°$.

Relationships between the contraction coeffcient C_c and $\frac{y_C}{y_B}$ for various values of γ, where y_B and y_C are value of y at point B and C, are shown in Figure 8. For each gate inclination γ, C_c is found to be a decreasing function of the ratio $\frac{y_C}{y_B}$.

4.2.2 $0 < \gamma < 60^\circ$

To find numerical solutions of this case, it is required to set the value of θ in the neighborhood of the stagnation point to be $60^\circ - \gamma$, i.e. $\theta_1^U = \delta = 60^\circ - \gamma$. Typical free surface profile is shown in Figure 9 for $\gamma = 35^\circ$. However, for a given ϕ_C that corresponds with gate length L, solutions exist for the gate inclination γ greater than some critical value χ_L. This critical value χ_L depends on gate length L. For small γ, it is difficult to find the numerical solution because the free surface near upstream separation can no longer satisfy the prescribed local behavior at the stagnation point ($\eta = 120^\circ$).

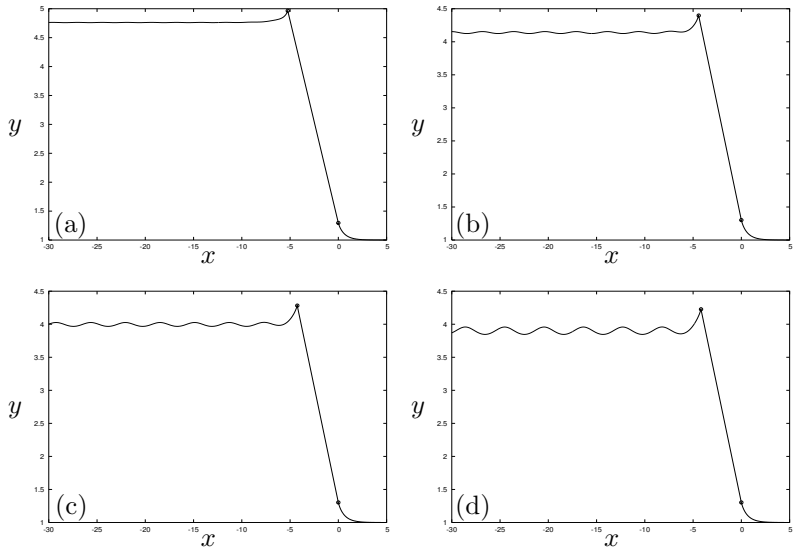

Figure 9: Profiles of the free surfaces and the gate when $\gamma = 35^\circ$: (a) $\phi_C = 2.00$, $F = 2.8161$ (b) $\phi_C = 1.70$, $F = 2.6066$ (c) $\phi_C = 1.60$, $F = 2.5622$ and (d) $\phi_C = 1.50$, $F = 2.5403$.

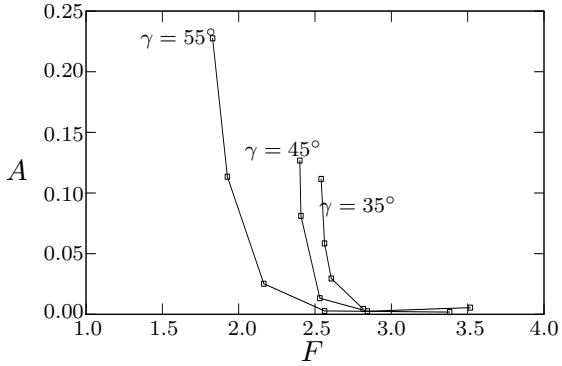

Figure 10: The amplitude A of the waves versus the Froude number F.

In Figure 10, it is shown that the amplitude of the waves increases as F decreases. For larger value of F, the upstream waves persist with finitely small amplitude. In addition, for a fixed value of F, these wave amplitude increases as the gate inclination decreases. Plots of numerical values of the contraction coefficient C_c versus $\frac{y_C}{y_B}$ for various values of γ are shown in Figure 11.

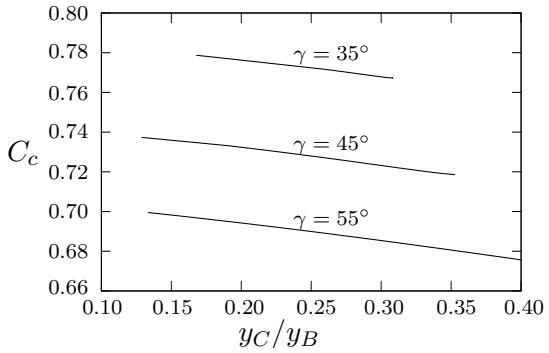

Figure 11: Values of the contraction coefficient C_c versus $\frac{y_C}{y_B}$.

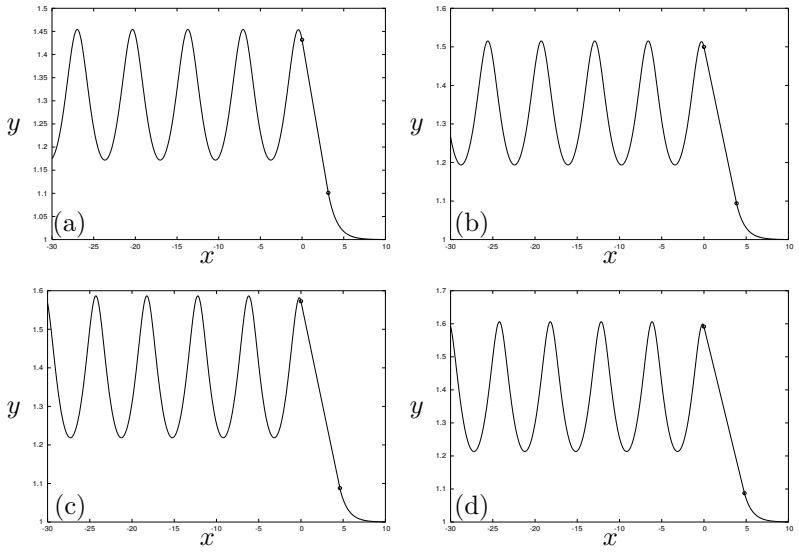

Figure 12: Profiles of the free surfaces and the gate when $\gamma = 6°$: (a) $\phi_C = 2.50$, $F = 1.2273$ (b) $\phi_C = 3.00$, $F = 1.2543$ (c) $\phi_C = 3.50$, $F = 1.2848$ and (d) $\phi_C = 3.618$, $F = 1.2897$.

5 Flows with smooth separations

In this case, we impose the following conditions $\theta_1^U = \delta = \theta_1^D = -\gamma$. These imply that the values of θ at both upstream and downstream separation points take on the value of gate inclination. Following the numerical scheme derived in sections 2 and 3, solutions are computed for various values of ϕ_C and γ. Most of the results are obtained with $N_1 = 636, N_2 = 801, \Delta_1 = 0.04$ and $\Delta_2 = 0.01$. Asavanant and Vanden-Broeck (1996) found solutions of this case for small gate inclination with limited values of downstream Froude number. Their solutions contain no waves on the upstream free surface due to some constraints of the numerical technique. Here we show that there exist solutions with upstream waves for larger values of gate inclination. The upper bound of gate inclination is found to depend on ϕ_C. For example, 9° when $\phi_C = 2.00$. Typical free-surface profile is shown in Figure 12 (a) - (d) for $\gamma = 6°$. The upstream waves tend to develop narrow crests and broad troughs showing the effect of nonlinearity as F increases.

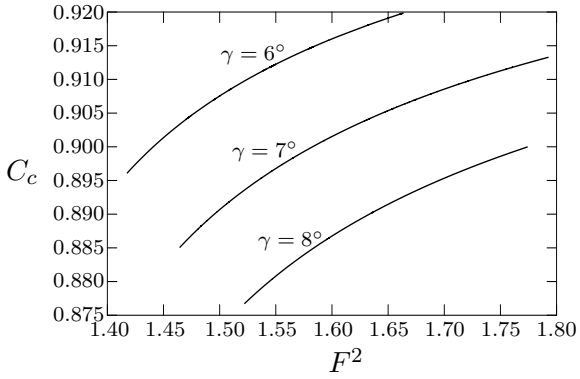

Figure 13: Values of contraction coefficient C_c versus F^2.

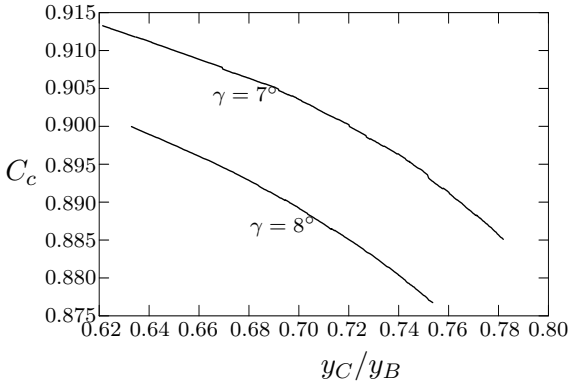

Figure 14: Values of contraction coefficient C_c versus $\frac{y_C}{y_B}$.

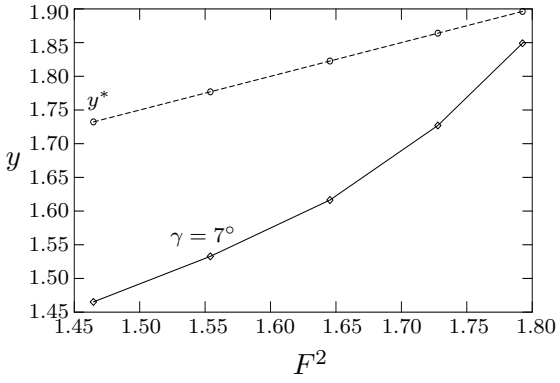

Figure 15: Numerical value of y at waves crests versus F^2. Dashed line represents the maximum elevation $y^* = \frac{F^2}{2} + 1$ is.

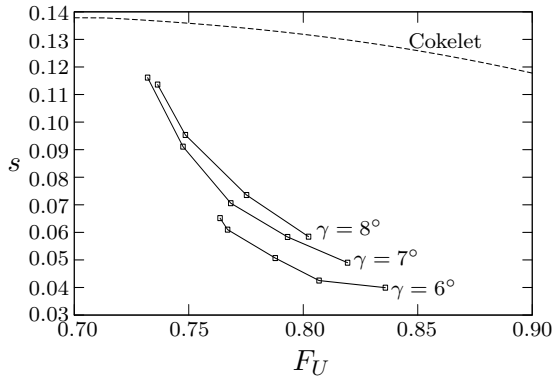

Figure 16: The steepness s of the waves versus the upstream Froude number F_U. The dashed curve corresponds the limiting cases characterized by a 120° angle at the crests (Cokelet 1977).

Numerical values of the contraction coefficient C_c and F^2 are shown in Figure 13. The contraction coefficient C_c is an increasing function of F^2 for a fixed value of γ. However the contraction coefficient C_c increases as the ratio of y_C and y_B decreases (see Figure 14). As F^2 increases, the level of wave crests approaches the highest level y^* of the free surface, i.e., $y^* = \frac{F^2}{2} + 1$ (see Figure 15).

In addition, steepness s of the waves, defined as ratio of the wave height and the wavelength, is shown to be a decreasing function of the upstream Froude number F_U as shown in Figure 16. Here F_U is defined as

$$F_U = \frac{V}{\sqrt{gD}},$$

where V is the average upstream velocity and D is the average upstream depth.

The Froude numbers F and F_U are related by

$$F_U^2 = \frac{F^2}{8}\left[\left(\frac{8}{F^2}+1\right)^{\frac{1}{2}} - 1\right]^3 .$$

As F_U decreases to the critical value F_U^*, the elevation of the crests tends to the maximum level $\frac{F_U^{*2}}{2}+1$ and the waves reach their limiting configuration characterized by a 120° angle at the crests (see Figure 16).

6 Conclusions

We have presented accurate numerical solutions of the free-surface flows under an inclined gate by using boundary integral method. The results show that there is a two-parameter family of solutions for which the parameters are the gate inclination γ and ϕ_C.

When the upstream separation is a stagnation point, the contact angle between the upstream free surface and the gate can be varied between 90° to 120° depending on the gate inclination γ. Solutions of the vertical gate ($\gamma = 90^\circ$) are computed and compared with previous results. This constitutes a check on the numerical scheme. For inclined gate with a stagnation point, it is found that numerical solutions exist for all value of $\gamma \in (\chi_L, 90^\circ)$. Here χ_L is the lower bound of the gate inclination and its value depends on ϕ_C or gate length L. Amplitude of the upstream waves appears to be a decreasing function of ϕ_C or the downstream Froude number F for a given γ. For large F, amplitude of the waves is finitely small and cannot be visually seen in the figure. In addition, the contraction coefficient C_c and gate length L decrease as F decreases.

Finally, we consider the inclined gate problem under which the free surfaces leave tangentially at both separation points. Numerical solutions for this case showed that there also exists a train of nonlinear waves on the upstream free surface. These solutions can be found for small gate inclination because of insufficient mesh points in the neighbourhood of the upstream separation point. It is observed from the local behavior of flow near the upstream separation point that, ultimately, the flow would satisfy the tangential separation condition. In addition, as the upstream Froude number F_U decreases, amplitude A and steepness s of the waves increase to the limiting values of Cokelet (1977). This case is thus required further investigation for large gate inclination.

Acknowledgement(s) : This work was financially supported in parts by the University Development Commission (U.D.C.) Scholarship and Chulalongkorn University's Research Division.

References

[1] J. Asavanat and J. M. Vanden-Broeck, Free-surface supercritical splashless flows past a two-dimensional symmetrical rectilinear body, *European J. Mech. B Fluids* 17 (1998), 811-822.

[2] J. Asavanant and J. M. Vanden-Broeck, Nonlinear free-surface flow emerging from vessels and flows under a sluice gate. *J. Austral. Math. Soc. Ser. B* 38 (1996), 63-86.

[3] G. K. Batchelor, An Introduction to Fluid Dynamics. Cambridge University Press, 1967.

[4] T. B. Benjamin, On the flow in channels when rigid obstacles are placed in the stream. *J. Fluid Mech.* 1 (1956), 227-248.

[5] B. J. Binder and J. M. Vanden-Broeck, Free surface flows past surfboards and sluice gates. *European J. Appl. Math.* 16 (2005), 601-619.

[6] E. D. Cokelet, Steep gravity waves in water of arbitrary uniform depth. *Philos. Trans. Roy. Soc. London Ser. A* 286 (1977), 183-230.

[7] G. Dagan and M. P. Tulin, Two-dimensional free-surface gravity flow past blunt bodies. *J. Fluid Mech.* 51 (1972), 529-543.

[8] A. Defina and F. M. Susin, Hysteretic behavior of the flow under a vertical sluice gate. *Phys. Fluids* 15 (2003), 2541-2548.

[9] D. D. Fangmeier and T. S. Strelkoff, Solution for gravity flow under a sluice gate. *ASCE J. Engrg. Mech. Div.* 94 (1968), 153-176.

[10] G. C. Hocking and J. M. Vanden-Broeck, Draining of a fluid of finite depth into a vertical slot. *Appl. Math. Modelling* 21 (1997), 634-649.

[11] J. H. Masliyah, K, Nandakumar, F. Hemphill and L. Fung, Body-fitted coordinates for flow under sluice gates. *ASCE J. Hydraulic Eng.* 111 (1985), 922-933.

[12] P. M. Naghdi and L. Vongsarnpigoon, Steady flow past a sluice gate. *Phys. Fluids* 29 (1986), 3962-3970.

[13] T. Petrila, Mathematical model for the free surface flow under a sluice gate. *Appl. Math. Comput.* 125 (2002), 49-58.

[14] J. M. Vanden-Broeck, Flow under a gate. *Phys. Fluids* 29 (1986), 3148-3151.

[15] J. M. Vanden-Broeck, Numerical calculations of the free-surface flow under a sluice gate. *J. Fluid Mech.* 330 (1997), 339-347.

[16] J. M. Vanden-Broeck and E. O. Tuck, E. O. Flow near the intersection of a free surface with a vertical wall. *SIAM J. Appl. Math.* 51 (1997), 1-13.

(Received 21 July 2008)

P. Guayjarernpanishk
Department of Mathematics
Faculty of Science
Chulalongkorn University
Bangkok 10330, THAILAND.
e-mail : gpanat@sci.ubu.ac.th

J. Asavanant
Advanced Virtual and Intelligent Computing (AVIC) Research Center
Faculty of Science
Chulalongkorn University
Bangkok 10330, THAILAND.
e-mail : jekjack@gmail.com